JOC Article
pubs.acs.org/joc

Theoretical Mechanistic Study of the TBD-Catalyzed Intramolecular Aldol Reaction of Ketoaldehydes

Peter Hammar,[†] Cynthia Ghobril,[‡] Cyril Antheaume,[‡] Alain Wagner,[‡] Rachid Baati,*[,‡] and Fahmi Himo*[,§]

[†]*Department of Theoretical Chemistry, School of Biotechnology, Royal Institute of Technology, SE-10691 Stockholm, Sweden,* [‡]*University of Strasbourg, Faculty of Pharmacy UMR/CNRS 7199, Laboratory of Functional ChemoSystem, 74, route de Rhin BP60024, 67401 Illkirch, France, and* [§]*Department of Organic Chemistry, Arrhenius Laboratory, Stockholm University, SE-10691 Stockholm, Sweden*

baati@bioorga.u-strasbg.fr; himo@organ.su.se

Received March 16, 2010

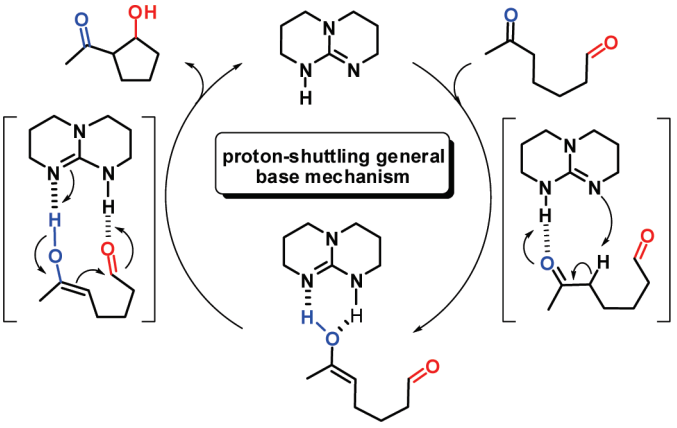

The intramolecular aldol reaction of acyclic ketoaldehydes catalyzed by 1,5,7-triazabicyclo-[4.4.0]dec-5-ene (TBD) is investigated using density functional theory calculations. Compared to the proline-catalyzed aldol reaction, the use of TBD provides a unique and unusual complete switch of product selectivity. Three mechanistic pathways are proposed and evaluated. The calculations provide new insights into the activation mode of bifunctional guanidine catalysts. In the favored mechanism, TBD first catalyzes the enolization of the substrate and then the C−C bond formation through two concerted proton transfers. In addition, the computationally predicted stereochemical outcome of the reaction is in agreement with the experimental findings.

I. Introduction

Over the past few years, many research efforts have focused on discovering new efficient and highly selective organocatalysts for C−C bond-forming reactions.[1] In particular, the versatility as well as the synthetic significance of the organocatalytic direct aldol reactions have been extensively studied and highlighted.[2] In the case of intermolecular aldolization, a great number of impressive milestones have been achieved for the control of both the regio- and enantioselectivity of the reaction.[3]

(1) (a) Paull, D. H.; Abraham, C. J.; Scerba, M. T.; Alde-Danfoth, E.; Lectka, T. *Acc. Chem. Res.* **2008**, *41*, 655–663. (b) Dalko, P., *Enantioselective Organocatalysis*; Wiley-VCH: Weinheim, 2007. (c) Buckley, B. R. *Annu. Rep. Prog. Chem., Sect. B* **2007**, *103*, 90–106. (d) Pellissier, H. *Tetrahedron* **2007**, *63*, 9267–9331. (e) Pihko, P. M. *Angew. Chem., Int. Ed.* **2006**, *45*, 544–547. (f) Gaunt, M. J.; Johansson, C. C. C.; McNally, A.; Vo, N. T. *Drug Discovery Today* **2007**, *12*, 8–27. (g) Jaroch, S.; Weinmann, H.; Zeitler, K. *ChemMedChem* **2007**, *2*, 1261–1264. (h) Ikunaka, M. *Org. Proc. Res. Dev.* **2007**, *11*, 495–502. (i) Dalko, P. I.; Moisan, L. *Angew. Chem., Int. Ed.* **2001**, *20*, 3726–3748.

(2) (a) Mitsui, K.; Hyatt, S. A.; Turner, D. A.; Hadad, C. M.; Parquette, J. R. *Chem. Commun.* **2009**, 3261–3263. (b) Wu, X.; Ma, Z.; Ye, Z.; Qian, S.; Zhao, G. *Adv. Synth. Catal.* **2009**, *351*, 158–162. (c) Adachi, S.; Harada, T. *Eur. J. Org. Chem.* **2009**, *22*, 3661–3671. (d) Evans, D. A. In *Modern Aldol Reactions*; Mahrwald, R., Ed.; Wiley-VCH: New York, 2004; Vol. 1. (e) List, B. *Chem. Rev.* **2007**, *107*, 5471–5569. (f) List, B. *Tetrahedron* **2002**, *58*, 5573–5590. (g) Alcaide, B.; Almendros, P. *Eur. J. Org. Chem.* **2002**, 1595–1601 and references cited therein. (h) Denmark, S. E.; Stavenger, R. A. *J. Am. Chem. Soc.* **2000**, *122*, 8837–8847. (i) Guillena, G.; Najera, C.; Ramon, D. J. *Tetrahedron: Asymmetry* **2007**, *18*, 2249–2293.

Published on Web 06/15/2010 DOI: 10.1021/jo100488g

SCHEME 1. Intramolecular Aldol Reaction of Ketoaldehydes Catalyzed by Proline and TBD

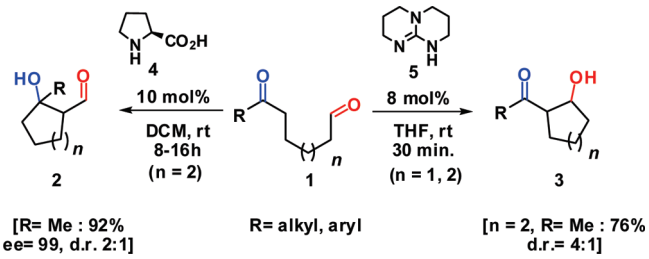

Despite these great advances, direct intramolecular aldol reaction of dialdehydes, ketoaldehydes, or diketones has received only a little attention, and few general methodologies have been reported that allow complete control of the regioselectivity and enantioselectivity of the cyclization. Only recently the control of regioselectivity for dicarbonyl substrates has been achieved with high enantioselection when proline catalysis is used under kinetic control (Scheme 1).[4,5] The successful implementation of the covalent enamine−iminium catalysis strategy allowed asymmetric *6-enolexo* aldolization of unmodified dicarbonyl systems giving rise to cyclic β-hydroxy carbonyls.[4] To date, the control of the regioselectivity for direct aldolization of unsymmetrical dicarbonyl substrates still stands as a challenge of paramount importance, since this strategy represents one of the most efficient means of synthesizing five-, six-, and seven-membered rings.[2d,5] In this context, we discovered recently that bifunctional guanidine catalysts, such as 1,5,7-triazabicyclo-[4.4.0]dec-5-ene (TBD), are powerful organocatalysts that promote regioselective direct 5- and 6-*enolexo* intramolecular aldolization of ketoaldehydes affording cyclic β-hydroxy ketones (Scheme 1).[6] The reactions performed with 8 mol % of TBD in THF at room temperature were complete after only 30 min and yielded 2-ketocyclopentanols and 2-ketocyclohexanols **3** in good to excellent yields as chromatographically separable *trans*/*cis* diastereoisomers.[6] Alternatively, such isomers could also be prepared in an indirect intramolecular aldol reaction of masked ketoaldehydes. However, these protocols are limited due to lengthy multistep procedures.[7] The unique activation mode of the TBD catalyst thus allows the formation of the adduct with a complete switch of product selectivity compared to the proline-catalyzed direct intramolecular aldolization of ketoaldehydes.[5] In that sense, this approach diverges from the later one and represents a promising endeavor in organocatalysis for the development and discovery of TBD-derived chiral catalysts. The origin of this inverted regioselectivity and the *trans*/*cis* diastereoselectivity of this transformation are challenging issues that still remain to be understood. While the reaction mechanism of the TBD-catalyzed direct aldolization of ketoaldehydes is unknown, a plausible mechanism has been recently postulated that relies on the dual properties of guanidines, namely their nucleophilicity and their strong basicity.[8] The efficiency of the TBD-catalyzed direct aldol reactions combined with the broad scope of applicability[6] prompted us to study in more detail the mechanism of this reaction in order to rationalize the stereochemical outcomes and to provide new insights into the unique activation mode of TBD.

In this study, three mechanistic possibilities have been envisioned for this reaction as depicted in Scheme 2. The first mechanism is a general base mechanism (pathway A, Scheme 2) where TBD first acts as a base to deprotonate the methylene group α to the ketone. In the following step, TBD acts as an acid to protonate the alkoxide form of the product, after the C−C bond formation.

The second mechanism (pathway B, Scheme 2) is a nucleophile mechanism, since it involves a covalent intermediate between the ketoaldehyde substrate and the catalyst. This suggestion was recently put forward and is based on the nucleophilic properties of guanidines.[6] It is inspired by the recent findings reported by Waymouth and Mioskowski, who studied the TBD-catalyzed polymerization of cyclic esters[9] and the aminolysis of esters,[10] respectively.

Finally, the third mechanism (pathway C, Scheme 2) is an enamine mechanism, which is based on the formation of a reactive enamine intermediate between TBD and the ketone. The enamine attacks the electrophilic aldehyde carbonyl, leading to the addition product. This is similar to the mechanism found for an array of pyrrolidine-catalyzed aldol-like reactions.[11]

We have investigated the energetic plausibility of these three reaction mechanisms by means of density functional theory (DFT) calculations. This approach is well-documented for the rationalization and the quantitative prediction of stereoselectivity in organocatalytic reactions.[11,12] In particular, DFT calculations have recently been successfully employed to study various mechanistic aspects of

(3) (a) Reis, O.; Eymur, S.; Reis, B.; Demir, A. S. *Chem. Commun.* **2009**, 1088–1090. (b) Nakayama, K.; Maruoka, K. *J. Am. Chem. Soc.* **2008**, *130*, 17666–17667. (c) Zhou, J.; Wakchaure, V.; Kraft, P.; List, B. *Angew. Chem., Int. Ed.* **2008**, *47*, 7656–7658. (d) Ogawa, S.; Shibata, N.; Nakamura, S.; Toru, T.; Shiro, M. *Angew. Chem., Int. Ed.* **2007**, *46*, 8666–8669. (e) Kano, T.; Yamaguci, Y.; Tanaka, Y.; Maruoka, K. *Angew. Chem., Int. Ed.* **2007**, *46*, 1738–1740. (f) Huang, J.; Zhang, X.; Armstrong, D. W. *Angew. Chem., Int. Ed.* **2007**, *46*, 9073–9077. (g) Tang, Z.; Marx, A. *Angew. Chem., Int. Ed.* **2007**, *46*, 7297–7300. (h) Hayashi, Y.; Sumiya, T.; Takahashi, J.; Gotoh, H.; Urushima, T.; Shoji, M. *Angew. Chem., Int. Ed.* **2006**, *45*, 958–961. (i) Mase, N.; Nakai, Y.; Ohara, N.; Yoda, H.; Takabe, K.; Tanaka, F.; Barbas, C. F., III. *J. Am. Chem. Soc.* **2006**, *128*, 734–735.

(4) Pidathala, C.; Hoang, L.; Vignola, N.; List, B. *Angew. Chem., Int. Ed.* **2003**, *42*, 2785–2788.

(5) (a) Itagaki, N.; Kimura, M.; Sugahara, T.; Iwabuchi, Y. *Org. Lett.* **2005**, *19*, 4185–4188. (b) Corey, E. J.; Ishiguro, M. *Tetrahedron Lett.* **1979**, 2745. (c) Heathcock, C. H.; Tice, C. M.; Germroth, T. C. *J. Am. Chem. Soc.* **1982**, *104*, 6081. (d) Enders, D.; Niemer, O.; Strasver, L. *Synlett* **2006**, 3399–3402. (e) Lalande, R.; Moulines, J.; Duboudin, J. *Bull. Soc. Chim. Fr.* **1962**, 1087. (f) Grieco, P. A.; Ohfune, Y. *J. Org. Chem.* **1980**, *45*, 2251–2254. (g) Wright, J.; Drtina, G. J.; Roberts, R. A.; Paquette, L. A. *J. Am. Chem. Soc.* **1988**, *110*, 5806. (h) Murai, A.; Tanimoto, N.; Sakamoto, N.; Masamune, T. *J. Am. Chem. Soc.* **1988**, *110*, 1985–1986.

(6) Ghobril, C.; Sabot, C.; Mioskowski, C.; Baati, R. *Eur. J. Org. Chem.* **2008**, *24*, 4104–4108.

(7) (a) Baik, T.-G.; Luis, A. L.; Wang, L.-C.; Krische, M. J. *J. Am. Chem. Soc.* **2001**, *123*, 5112–5113. (b) Jang, H.-Y.; Huddleston, R. R.; Krische, M. J. *J. Am. Chem. Soc.* **2002**, *124*, 15156–15157. (c) Nokami, J.; Mandai, T.; Watanabe, H.; Ohyama, H.; Tsuji, J. *J. Am. Chem. Soc.* **1989**, *111*, 4126–4127.

(8) (a) Coles, M. P. *Chem. Commun.* **2009**, 3659–3676. (b) Leow, D.; Tan, C.-H. *Chem. Asian J.* **2009**, *4*, 488–507.

(9) (a) Pratt, R. C.; Lohmeijer, B. G. G.; Long, D. A.; Waymouth, R. M.; Hendrick, J. L. *J. Am. Chem. Soc.* **2006**, *128*, 4556–4557. (b) Lohmeijer, B. G. G.; Pratt, R. C.; Leibfarth, F.; Logan, J. W.; Long, D. A.; Dove, A. P.; Nederberg, F.; Choi, J.; Wade, C.; Waymouth, R. M.; Hedrick, J. L. *Macromolecules* **2006**, *39*, 8574–8583.

(10) Sabot, C.; Kanduluru, A. K.; Meunier, S.; Mioskowski, C. *Tetrahedron Lett.* **2007**, *48*, 3863–3866.

(11) (a) Rankin, K. N.; Gauld, J. W.; Boyd, R. J. *J. Phys. Chem. A* **2002**, *106*, 5155–5159. (b) Arnó, M.; Domingo, L. R. *Theor. Chem. Acc.* **2002**, *108*, 232–239. (c) Clemente, F. R.; Houk, K. N. *Angew. Chem., Int. Ed.* **2004**, *43*, 5766–5768.

SCHEME 2. Possible Mechanisms for the Intramolecular Aldol Reaction Catalyzed by TBD Considered in the Present Study

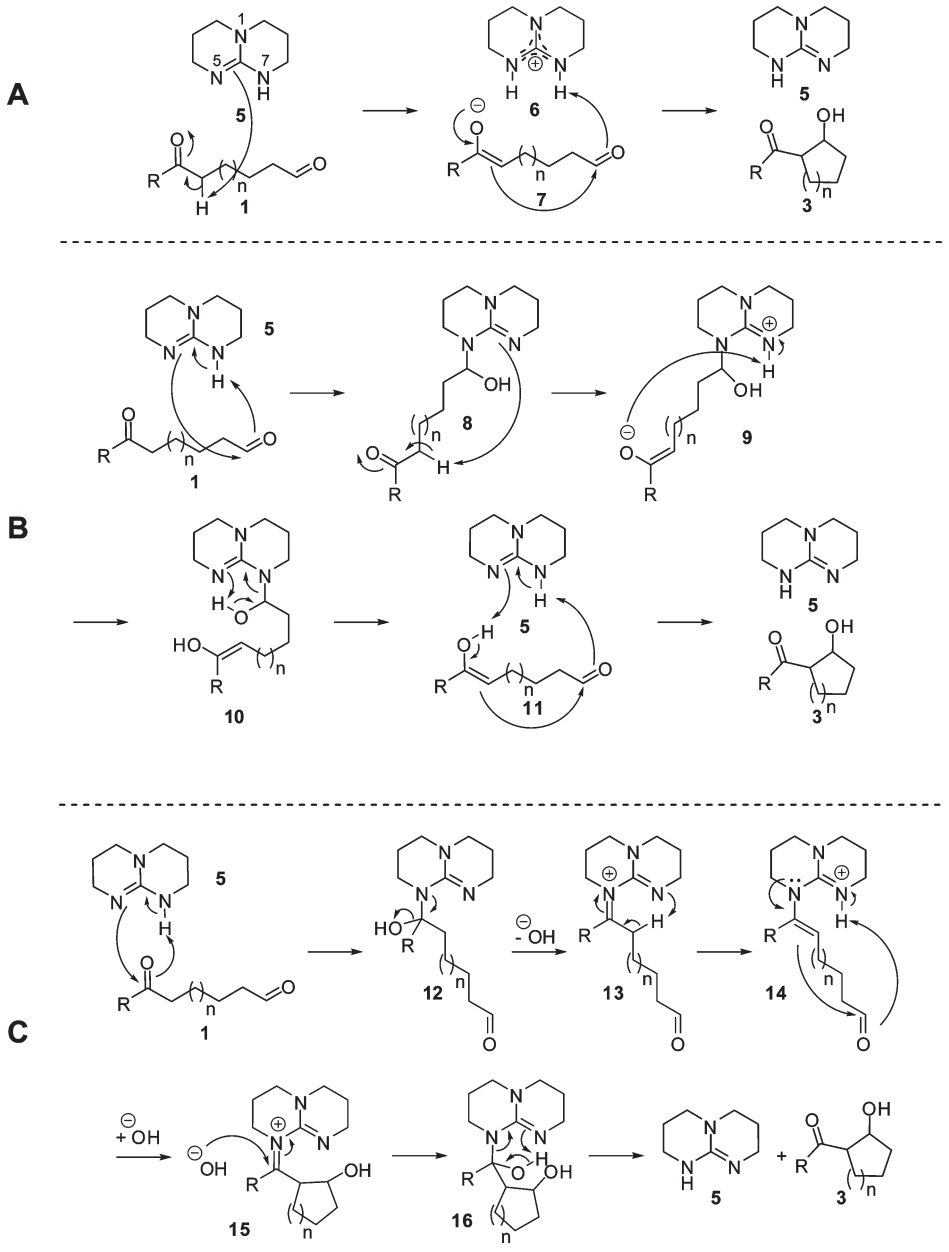

guanidine-catalyzed reactions, such as ring-opening polymerization of cyclic esters,[13] hydrolysis of acetonitrile,[14] and addition of fluorocarbon nucleophiles and *N*-alkyl maleimides.[15]

II. Computational Details

Calculations have been performed using the B3LYP[16] density functional method as implemented in the Gaussian03 program package.[17] Geometries were optimized using the 6-31G(d,p) basis set. Energies were then calculated as a single points with the larger 6-311+G(2d,2p) basis set. Frequencies were calculated at the same level as the geometry optimization to verify the nature of the stationary points and to obtain zero-point vibrational corrections. Solvation effects were also calculated as single points at the same level as the geometry optimization using the CPCM method.[18] The parameters of THF were used, since it was the solvent used in the experiments. Only

(12) (a) Allemann, C.; Gordillo, R.; Clemente, F. R.; Cheong, P. H.-Y.; Houk, K. N. *Acc. Chem. Res.* **2004**, *37*, 558–569. (b) Bahmanyar, S.; Houk, K. N.; Martin, H. J.; List, B. *J. Am. Chem. Soc.* **2003**, *125*, 2475–2479. (c) Hammar, P.; Córdova, A.; Himo, F. *Tetrahedron: Asymmetry* **2008**, *19*, 1617–1621. (d) Bassan, A.; Zou, W.; Reyes, E.; Himo, F.; Córdova, A. *Angew. Chem., Int. Ed.* **2005**, *44*, 7028–7032. (e) Marcelli, T.; Hammar, P.; Himo, F. *Chem.—Eur. J.* **2008**, *14*, 8562–8571.

(13) (a) Chuma, A.; Horn, H. W.; Swope, W. C.; Pratt, R. C.; Zhang, L.; Lohmeijer, B. G. G.; Wade, C. G.; Waymouth, R. M.; Hedrick, J. L.; Rice, J. E. *J. Am. Chem. Soc.* **2008**, *130*, 6749–6754. (b) Simón, L.; Goodman, J. M. *J. Org. Chem.* **2007**, *72*, 9656–9662.

(14) Ma, J.; Zhang, X.; Zhao, N.; Xiao, F.; Wei, W.; Sun, Y. *THEOCHEM* **2009**, *911*, 40–45.

(15) Jiang, Z.; Pan, Y.; Zhao, Y.; Ma, T.; Lee, R.; Yang, Y.; Huang, K.-W.; Wong, M. W.; Tan, C.-H. *Angew. Chem., Int. Ed.* **2009**, *48*, 3627–3631.

(16) (a) Becke, A. D. *J. Chem. Phys.* **1993**, *98*, 5648–5652. (b) Becke, A. D. *Phys. Rev. A* **1988**, *38*, 3098–3100. (c) Vosko, S. H.; Wilk, L.; Nusair, M. *Can. J. Phys.* **1980**, *58*, 1200–1211. (d) Lee, C.; Yang, W.; Parr, R. G. *Phys. Rev. B* **1988**, *37*, 785–789.

(17) *Gaussian 03*, Revision D.01; Gaussian, Inc.: Wallingford, CT, 2004.

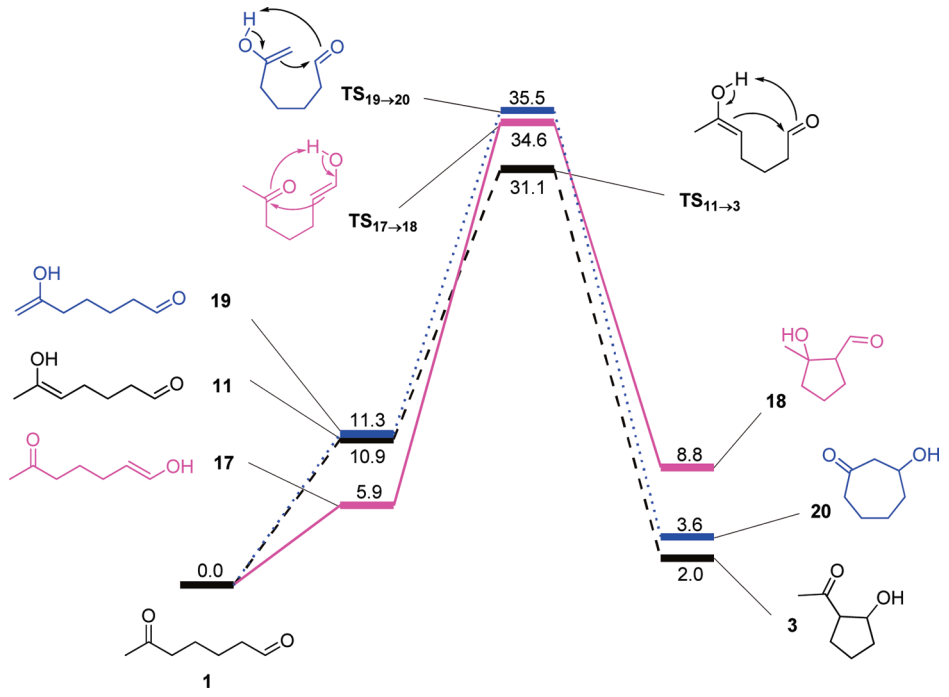

FIGURE 1. Potential energy profile for the uncatalyzed reaction, energies in kcal/mol including solvation in THF.

SCHEME 3. Possible Cyclization Products Allowed by Baldwin Rules

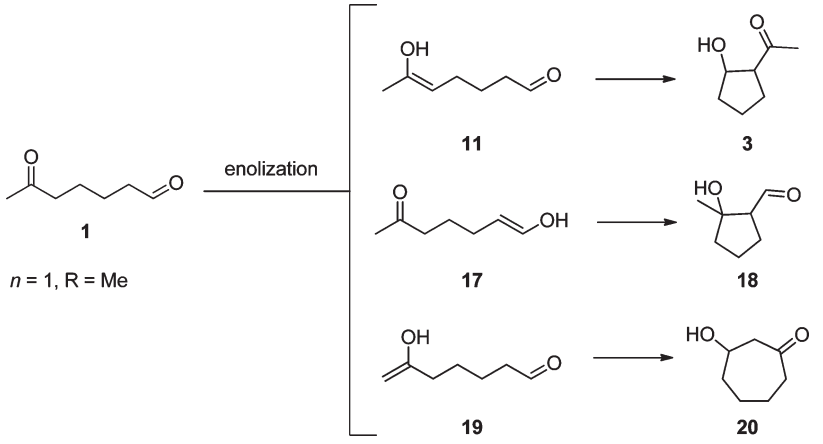

electrostatic contributions were included from the CPCM calculations. The energies reported here are thus the energies obtained with the large basis set to which the zero-point energies and solvation effects were added.

III. Results and Discussion

In this section, we first discuss the results of the calculations concerning the uncatalyzed reaction. We then focus on the various proposals for the TBD-catalyzed reaction. At the end we discuss the results regarding the diastereoselectivity of the reaction.

III. A. Uncatalyzed Reaction. Before discussing the results for the TBD-catalyzed reaction, it is instructive to consider the uncatalyzed case.

In order to achieve the C−C bond formation, ketoaldehyde **1** has to enolize first. As shown in Scheme 3, three different enolization products can be formed, leading to the three different cyclization products allowed by the Baldwin rules.[19] Enol **11**, which leads to the experimentally observed regioisomer **3**, is calculated to be 10.9 kcal/mol higher than **1**, while enols **17** and **19** are 5.9 and 11.3 kcal/mol higher than **1**, respectively. These values agree quite well with results in the literature.[20] However, although the enol forms are energetically accessible, previous studies have shown that the barrier for enolization (e.g., **1**→**11**) in the absence of an acid or a base could be as high as 60 kcal/mol.[20,21] As a consequence, and

(18) (a) Barone, V.; Cossi, M. *J. Phys. Chem. A* **1998**, *102*, 1995–2001. (b) Cossi, M.; Rega, N.; Scalmani, G.; Barone, V. *J. Comput. Chem.* **2003**, *24*, 669–681.

(19) (a) Baldwin, J. E. *J. Chem. Soc., Chem. Commun.* **1976**, *18*, 734–736. (b) Baldwin, J. E.; Lusch, M. J. *Tetrahedron* **1982**, *38*, 2939–2947.

(20) (a) Lee, D.; Kim, C. K.; Lee, B.-S.; Lee, I.; Lee, B. C. *J. Comput. Chem.* **1997**, *18*, 56–69. (b) Zhang, X.; Houk, K. N. *J. Org. Chem.* **2005**, *70*, 9712–9716. (c) Smith, B. J.; Tho, N. M.; Bouma, W. J.; Radom, L. *J. Am. Chem. Soc.* **1991**, *113*, 6452–6458.

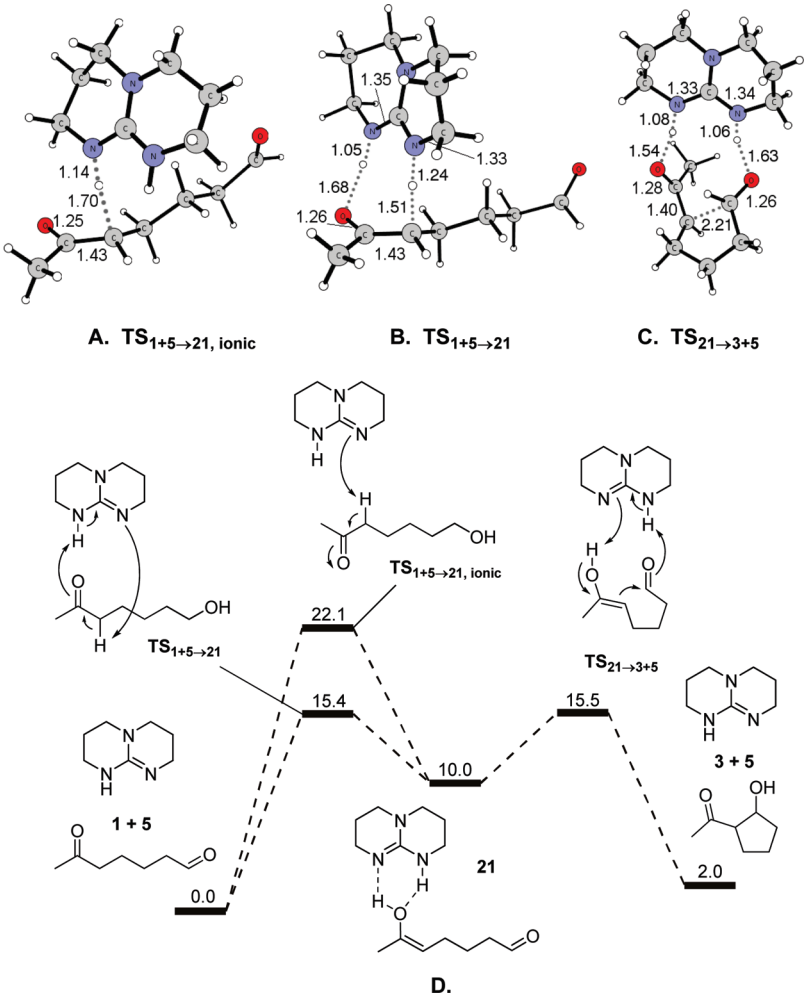

FIGURE 2. (A) Optimized transition state for the proton abstraction. (B) Transition state for proton shuttling enolization. (C) C−C bond formation transition state with concerted proton shuttling. Relevant distances are given in Å. (D) Potential energy graph for the base mechanism. Energies are given in kcal/mol including solvation effects.

due to the fact that adducts **18** and **20** have not been observed in our experimental conditions, computations were carried out considering enol **11**.

We have also located transition states for the ring-closing reactions of the three enols leading to the different regioisomers. The results are shown in Figure 1 (optimized structures are given in the Supporting Information). In all three cases, the transition states involve the transfer of the enol proton to the aldehyde concomitant with the C−C bond formation. The lowest overall barrier is calculated to be for the reaction leading to regioisomer **3** (31.1 kcal/mol). The transition states leading to the other regioisomers have slightly higher energies, 34.6 and 35.5 kcal/mol for $\mathbf{TS_{17\rightarrow 18}}$ and $\mathbf{TS_{19\rightarrow 20}}$, respectively. The aldol products **3**, **18**, and **20** are calculated to be 2.0, 8.8, and 3.6 kcal/mol, respectively, higher than ketoaldehyde **1**.

Based on the results of the uncatalyzed reaction it is clear that the mechanism of the TBD-catalyzed reaction has to achieve two important tasks. The barrier for the initial enolization step has to be greatly reduced or somehow circumvented and the barrier for the C−C bond formation step has to be lowered significantly. The mechanism has also to be able to rationalize the observed regioselective outcome of the catalyzed reaction.

III. B. General Base Mechanism. In the base mechanism (pathway A, Scheme 2), TBD first acts as a base to deprotonate the ketoaldehyde and in the subsequent step as an acid to protonate the alkoxide form of the product. We have here located the transition state for the proton abstraction step ($\mathbf{TS_{1+5\rightarrow 21,ionic}}$ shown in Figure 2A), and the barrier is calculated to be 22.1 kcal/mol. The resulting ion pair (enolate and protonated TBD) was not able to be optimized because it always collapsed to the neutral TBD-enol complex. This complex is calculated to be 10.0 kcal/mol higher than the reactants, which is quite close to the enolization energy found above (10.9 kcal/mol).

This barrier represents thus a huge reduction of the enolization barrier compared to the uncatalyzed case. However, a significantly lower barrier is found when the proton abstraction takes place concertedly with another proton transfer, from the other nitrogen to the enolate oxygen

(21) (a) Dickerson, T. J.; Lovell, T.; Meijler, M. M.; Noodleman, L.; Janda, K. D. *J. Org. Chem.* **2004**, *69*, 6603–6609. (b) Rodríguez-Santiago, L.; Vendrell, O.; Tejero, I.; Sodupe, M.; Bertran, J. *Chem. Phys. Lett.* **2001**, *334*, 112–118. (c) Coitiño, E. L.; Tomasi, J.; Ventura, O. N. *J. Chem. Soc., Faraday Trans.* **1994**, *90*, 1745–1755.

($\mathbf{TS_{1+5\rightarrow 21}}$, shown in Figure 2). The barrier for this reaction mode is calculated to be 15.4 kcal/mol. The transition state for the following C−C bond forming step ($\mathbf{TS_{21\rightarrow 3+5}}$ in Figure 2) was also located and was found to occur concertedly with the deprotonation of the enol and the protonation of the aldehyde, where the TBD catalyst acts as the proton shuttle. This transition state has a similar energy as the first step, namely 15.5 kcal/mol over the reactants. The overall potential energy profile is shown in Figure 2D. This concerted base mechanism thus lowers the barrier for ring formation by more than 15 kcal/mol compared to the uncatalyzed reaction.

Both steps of the reaction are hence significantly catalyzed by the availability of two nitrogen sites in the catalyst, providing a possibility for the described concerted proton shuttling. Further support for this mechanism can be found by considering that the methylated TBD derivative (MTBD), in which one of the nitrogen sites is blocked by a methyl group, is a less effective catalyst for the aldol reaction of **1** to give **3**, resulting in slow reaction kinetics (140 times slower than TBD) and lower yields of the adduct **3** (39% after 72 h of reaction time vs. 94% after 30 min).[6]

III. C. Nucleophile Mechanism. Inspired by the reports of Waymouth and Mioskowski, who studied the TBD-catalyzed polymerization of cyclic esters[9] and the aminolysis of esters,[10] respectively, a plausible covalent mechanism for the intramolecular aldolization of ketoaldehydes was previously proposed (pathway B, Scheme 2).[6] A very recent kinetic investigation by Waymouth on the acylation of amines by esters in the presence of TBD shows support for a nucleophilic mechanism.[22] Additional supports for this mechanism have been obtained by means of two-dimensional diffusion-ordered NMR spectroscopy (2D-DOSY) NMR that allows the analysis of distinct species in homogeneous solution on the basis of their specific diffusion rate.[23] Mass spectrometry represents also a powerful complementary tool that has been used for the analysis of the reaction mixture and detection of intermediates.[24]

The energetic plausibility of this mechanism is examined here. The reaction of **1** and **5** to give **8** has a calculated barrier of the very feasible 7.9 kcal/mol, and the covalent intermediate **8** is only 2.7 kcal/mol higher than the reactants. The optimized structure of $\mathbf{TS_{1+5\rightarrow 8}}$ is shown in Figure 3, and the energy profile for the reaction pathway is summarized in Figure 4.

To proceed, covalent intermediate **8** has to enolize. A transition state for intramolecular enolization, $\mathbf{TS_{8\rightarrow 10}}$, was optimized and is also shown in Figure 3. This is a quite peculiar transition state in which the α-proton is abstracted by the alcohol concertedly as the alcohol proton is transferred via the TBD nitrogen to the carbonyl. This structure is quite strained, leading to a reaction barrier of 24.1 kcal/mol compared to the free reactants. The resulting enol intermediate is +13.8 kcal/mol compared to the reactants. The barrier is thus considerably higher than for the concerted base mechanism described above (15.4 kcal/mol). An alternative way to achieve enolization is by introducing a second TBD molecule. In this case, the transition state and the barrier are very similar to the enolization step of the base mechanism discussed above. Indeed, the barrier is calculated to be 16.1 kcal/mol relative to **8**, and the enol intermediate lies at +11.1 kcal/mol (+18.8 and +13.8 kcal/mol, respectively, relative to reactants **1** + **5**). The optimized structure of the transition state ($\mathbf{TS_{8\rightarrow 10,\ 2\times TBD}}$) is also shown in Figure 3.

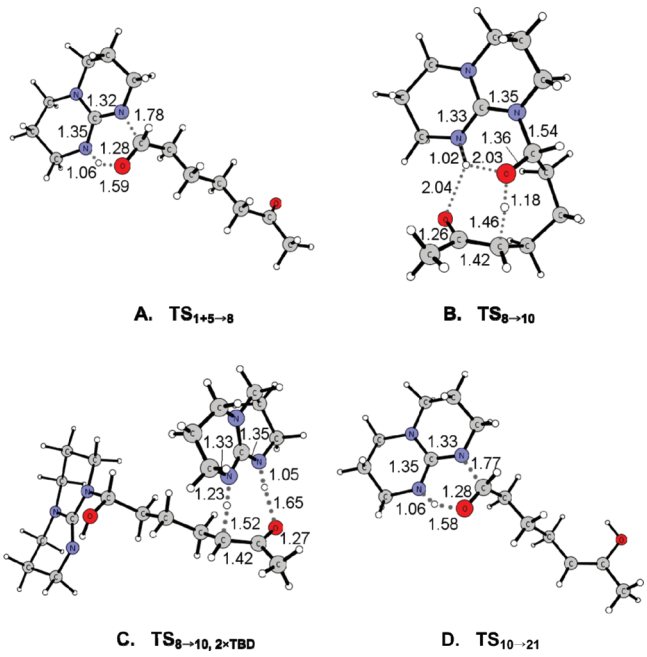

FIGURE 3. (A) Transition state for the formation of the covalent intermediate **8**. (B) Enolization transition state involving one TBD. (C) Enolization transition state on the covalent intermediate by a second TBD molecule. (D) Transition state for the dissociation of the covalent intermediate.

From **10**, the calculated overall barrier for breaking the covalent bond to the enol is calculated to be 18.9 kcal/mol ($\mathbf{TS_{10\rightarrow 21}}$, Figure 3), and the resulting intermediate, **21**, which is also found in the base mechanism, has an energy of 10.0 kcal/mol. TBD can then catalyze the final cyclization step in the same fashion as described for the base mechanism ($\mathbf{TS_{21\rightarrow 3+5}}$, Figure 2), with an accumulated barrier of 15.5 kcal/mol.

Thus, the difference between this mechanism and the base mechanism discussed above is in the steps leading to the formation of the enol intermediate **11**. Although the existence of intermediate **8** can be rationalized by the calculations, it is shown that the nucleophile mechanism provides no energetic advantage for the following enolization step as compared to the base mechanism. In particular, the requirement of two catalyst molecules makes this scenario less likely.

III. D. Enamine Mechanism. The third reaction mechanism considered here envisions the formation of a reactive enamine intermediate which attacks the aldehyde carbonyl leading to the aldol product (pathway C in Scheme 2). This is similar to the mechanism found for a number of pyrrolidine-catalyzed aldol-like reactions.[11]

The initial step of this mechanism is the formation of an *N*,*O*-hemiketal intermediate **12** by addition of TBD to the ketone. The barrier for this step is calculated to be 15.8 kcal/mol,

(22) Kiesewetter, M. K.; Scholten, M. D.; Kirn, N.; Weber, R. L.; Hedrick, J. L.; Waymouth, R. M. *J. Org. Chem.* **2009**, *74*, 9490–9496.
(23) Cohen, Y.; Avram, L.; Frish, L. *Angew. Chem., Int. Ed.* **2005**, *44*, 520.
(24) We have detected intermediate **8** by both 2D-DOSY NMR spectroscopy and mass spectrometry. Details are given in the Supporting Information

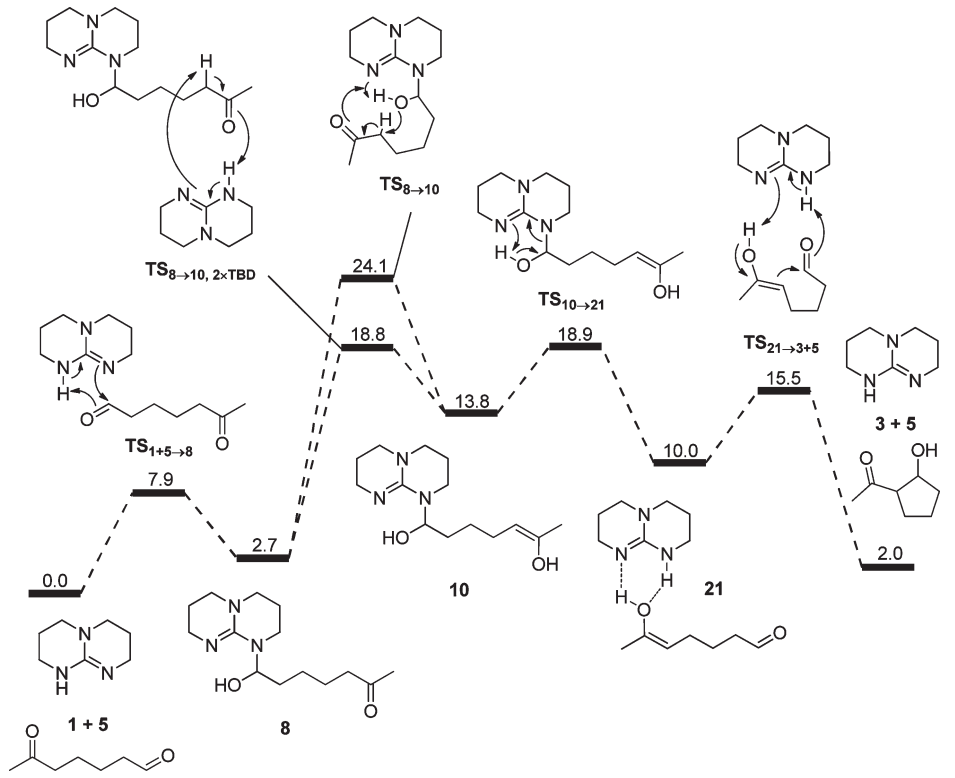

FIGURE 4. Potential energy profile for the nucleophile mechanism.

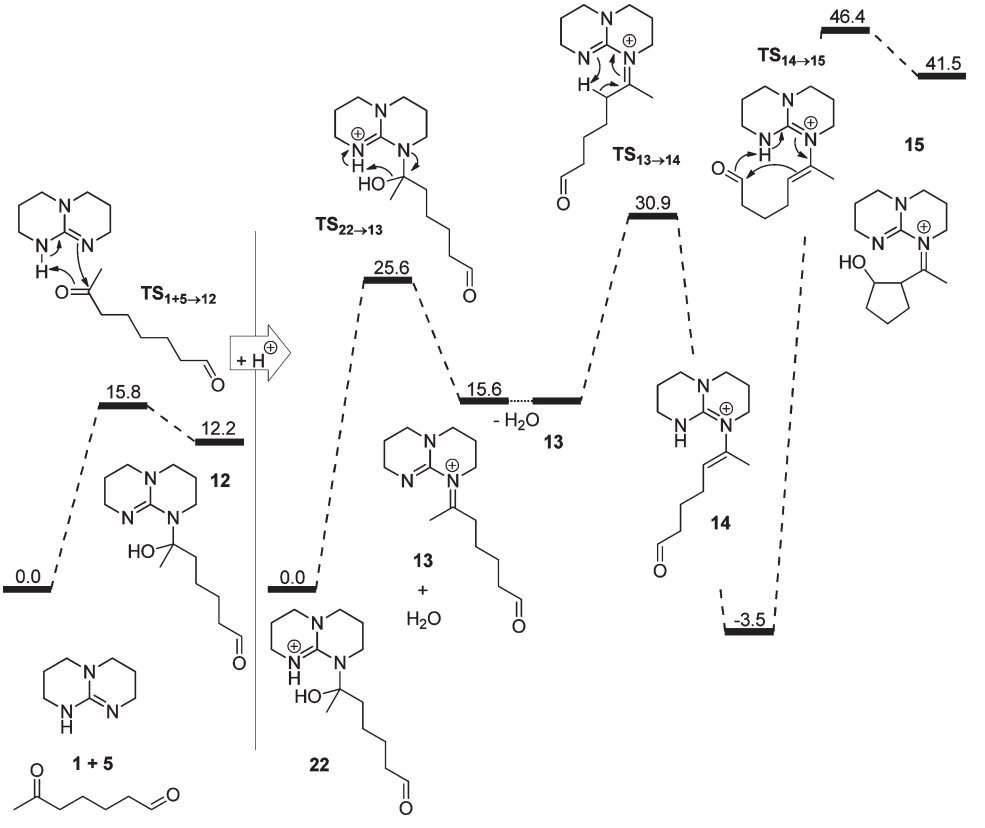

FIGURE 5. Potential energy profile for the enamine mechanism.

and intermediate **12** is calculated to be 12.2 kcal/mol higher than the reactants (see Figure 5). These energies are significantly higher than the corresponding ones for the analogous nucleophilic attack on the aldehyde discussed in the previous

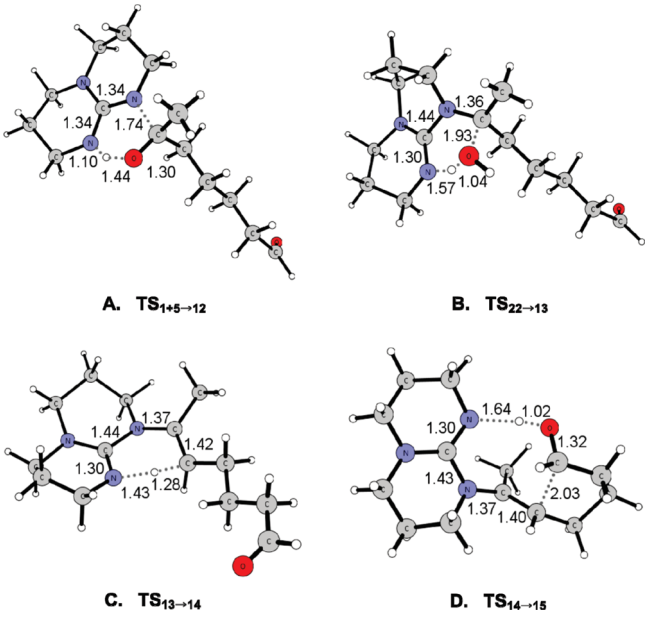

FIGURE 6. Optimized transition state structures along the enamine reaction mechanism: (A) Formation of the hemiketal, (B) Dehydration TS, (C) Iminium-enamine transformation, (D) C−C bond formation.

section (7.9 and 2.7 kcal/mol, respectively), but are comparable to the energies found for the initial step of the base mechanism. However, the following steps of the enamine mechanism are problematic from energetic point of view. First, the hemiketal intermediate **12** has to be protonated and there is no obvious proton source in the reaction medium (except perhaps the conjugated acid of the TBD catalyst). Even if we assume that the protonation step can be accomplished somehow, the calculations show that the following events are energetically prohibited (Figure 5). For example, the barrier for the water elimination in **22** is calculated to 25.6 kcal/mol and the intramolecular iminium−enamine transformation ($\mathbf{TS_{13\rightarrow 14}}$) has a barrier of 30.9 kcal/mol. Most importantly, the subsequent C−C bond formation step ($\mathbf{TS_{14\rightarrow 15}}$), which is coupled with a proton transfer from TBD, has a barrier as high as 49.9 kcal/mol. The energy profile for the enamine pathway is summarized in Figure 5 and optimized transition states along the pathway are displayed in Figure 6. The results shown here rule thus out this mechanism.

III. E. Diastereoselectivity. Product **3** is experimentally observed to be in a 3:1 mixture of the *trans*- and *cis*-diastereoisomers. However, kinetic NMR studies show that the formation of *cis*-**3** is faster, but that it readily transforms into the *trans* form (see the Supporting Information).

We have calculated the difference in energy between the two diastereoisomers of **3** to be 0.5 kcal/mol in favor of the *trans*-isomer, which is in a very good agreement with the observed ratio. Also in agreement with the experimental findings, the transition state for the formation of *cis*-**3** ($\mathbf{TS_{21\rightarrow}}$*cis*-$\mathbf{3+5}$ shown in Figure 7) is calculated to be 2.3 kcal/mol lower than the transition state for the formation of the *trans*-product ($\mathbf{TS_{21\rightarrow 3+5}}$ in Figure 2C). The preference of the *cis*-structure in the transition state is due to a more optimal alignment for the proton shuttling. The distance between the two oxygens is shorter allowing a more linear transfer of the protons to and from TBD.

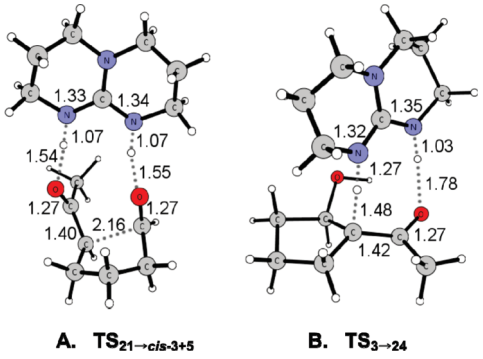

FIGURE 7. (A) Formation of the *cis*-**3** stereoisomer. (B) Transition state for tautomerization.

SCHEME 4. Possible Epimerization Mechanism

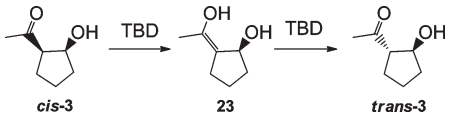

These results show thus that *cis*-**3** is the kinetic product, while *trans*-**3** is the thermodynamic product. The transformation between the two products can take place either via the reverse reaction (ring-opening catalyzed by TBD, i.e., *cis*-**3** + **5** → **21**) or by an epimerization mechanism. The former possibility has a barrier of 10.7 kcal/mol, which is obtained easily from the already available energies (15.5 − 2.0 − 2.3 − 0.5 = 10.7 kcal/mol).

To achieve epimerization, *cis*-**3** can first tautomerize to form enol **23** (Scheme 4). This can be achieved via a concerted proton shuttling mechanism with help of TBD, in a similar fashion as in the base mechanism discussed above. The optimized transition state for this is shown in Figure 7. The barrier is calculated to be 16.3 kcal/mol, which is somewhat higher than the ring-opening mechanism.

It should here be added that the alternative mechanism in which TBD only abstracts the proton from *cis*-**3** and delivers it back to yield the other diastereoisomer (i.e., without the formation of enol **23**) has an even higher barrier because the enolate-protonated TBD **6** ion pair is 18.9 kcal/mol higher than the neutral species, TBD + *cis*-**3**.

To summarize, the calculations show that it is possible to readily go between the two diastereoisomers, which can rationalize the observed diastereoselectivity.

IV. Conclusions

We have in the present paper investigated the reaction mechanism for the TBD-catalyzed intramolecular aldol reaction of ketoaldehydes. Three possible mechanisms were considered. The calculations show that TBD catalyzes the reaction through two steps. In the first step, a concerted proton abstraction/proton donation enolization of the ketoaldehyde takes place. In the second step, the C−C bond formation step occurs concertedly with proton transfers from the enol to the aldehyde, shuttled through the TBD catalyst. TBD thus acts as a bifunctional catalyst in which the two available nitrogen sites are crucial for the reaction. For the alternative nucleophile mechanism it is shown that the

formation of a covalent intermediate between TBD and the substrate does not provide any catalytic effect in the reaction. Also, the enamine mechanism which is analogous to the mechanism of amino acid-catalyzed aldol reaction is ruled out by the calculations.

These findings are in line with the mechanistic results of other guanidine-catalyzed reactions. For example, the TBD-catalyzed ring-opening polymerization of cyclic esters has computationally been shown to go through a hydrogen-bonded pathway rather than a covalently bound one as originally proposed.[13] Also, the mechanism of the stereoselective addition of fluorocarbon nucleophiles and *N*-alkyl maleimides using the chiral bicyclic guanidine 3,7-di-*tert*-butyl-1,4,6-triazabicyclo[3.3.0]oct-4-ene was found to proceed via proton transfer to the guanidine and coordination of the reacting species by hydrogen bonding with the guanidinium ion.[15] Furthermore, in the TBD-catalyzed hydrolysis of acetonitrile, a computationally feasible mechanism involves a number of steps consisting of both stepwise and concerted proton transfers.[14]

Finally, in addition to the mechanistic study, the calculations presented in the current study rationalize the experimentally observed stereochemical outcome of the reaction.

Acknowledgment. F.H. gratefully acknowledges the Swedish Research Council (VR) for financial support. This work has been supported by the Swedish National Infrastructure for Computing via PDC. R.B. is grateful to the Ministère Délégué à l'Enseignement Supérieur et à la Recherche for a grant to C.G. and to the CNRS for financial support. Dr. Lionel Allouche (NMR facility, University of Strasbourg) and Dr. Patrick Wehrung (Service Commun d'Analyses, Faculty of Pharmacy) are also acknowledged for fruitful discussions on 2D-DOSY NMR and MS analysis, respectively.

Supporting Information Available: Optimized structures for uncatalyzed reaction; 2D-DOSY NMR spectra and MS spectra for the identification of intermediate **8**; kinetic studies on the diastereoselectivity performed by ^{1}H NMR spectroscopy; absolute energies and Cartesian coordinates of optimized structures. This material is available free of charge via the Internet at http://pubs.acs.org.